Resonance phenomena in electron scattering by atomic oxygen from 9 to 11.4 eV

Y. Wang and Y. Zhou*
Center for Theoretical Atomic and Molecular Physics, Academy of Fundamental and Interdisciplinary Sciences, Harbin Institute of Technology, Harbin 150080, People's Republic of China

K. Ratnavelu
Institute of Mathematical Sciences, University of Malaya, Kuala Lumpur 50603, Malaysia
(Received 22 July 2010; published 30 September 2010)

The momentum-space coupled-channels optical method has been used to study negative-ion resonance phenomena in electron impact on atomic oxygen in the energy region of 9–11.4 eV. Total scattering cross sections have been calculated, and negative-ion resonances have been located. Most of the known resonances of available experimental observations and theoretical results have been confirmed, and some new resonance features have been found in the present calculation.

DOI: 10.1103/PhysRevA.82.034702 PACS number(s): 34.80.Dp, 34.80.Bm

I. INTRODUCTION

Negative-ion resonance phenomena in electron impact on atoms is a fundamental process in plasma physics, astrophysics, and the physics of the upper atmosphere. Study of its formation has been a focal subject in the past few decades due to its extreme sensitivity to the electron correlation effects [1,2]. The oxygen atom is one of the most abundant elements in the atmosphere, and studies of its negative-ion (O^-) resonances have been carried out since the 1970s. Edwards *et al.* [3,4] first observed the experimental evidence for autodetaching states of O^- at 9.5 and 10.87 eV with the configurations of $2p^3(^4S^o)3s3p\ ^2P$ and $2p^3(^4S^o)3p^2\ ^2P^o$ in keV collisions of O^- with atoms such as He, Ne, and Ar. Subsequently, Spence [5] observed resonances in electron scattering by atomic oxygen at 10.73 and 10.90 eV belonging to the configurations of $2p^3(^4S^o)3p^2\ ^6P^o$ and $2p^3(^4S^o)3p^2\ ^2P^o$, respectively. On the theoretical side, Matese *et al.* [6,7] predicted resonance positions at 9.5, 10.63, and 10.88 eV, which belong to the configurations of $2p^3(^4S^o)3s3p\ ^2P$, $2p^3(^4S^o)3p^2\ ^6P^o$, and $2p^3(^4S^o)3p^2\ ^2P^o$, respectively, in their configuration-interaction calculations. Rountree and Henry [8] found two broader resonance structures at 9.67 and 9.94 eV in the ^2P and ^4P channels in their calculated $2p^4\ ^3P$–$2p^3 3s\ ^3S^o$ excitation cross sections of electron-oxygen collision. A comprehensive review of previous studies can be found in the article of Buckman and Clark [2]. However, the known resonances may be still fewer than there should be, as they consist primarily of low-lying doubly excited states associated with the various terms of the grandparent $O^+\ 2p^3$ ion core. This insufficiency has motivated us to investigate the resonance phenomena in electron-oxygen (e-O) collisions at energies a few eV below the ionization threshold of atomic oxygen. This Brief Report demonstrates an investigation of negative-ion resonances in e-O collisions in the energy region from 9 to 11.4 eV. Most of the known resonances are confirmed and some new resonance features are found in the present calculation.

The present calculation has been carried out by employing the momentum-space coupled-channels optical (CCO) method. The CCO method has been applied for more than two decades in studies of electron collisions with atoms [9–16]. A distinct feature of the CCO method is that it uses an *ab initio* equivalent local optical potential to describe the continuum of target. The real part of the potential represents polarization of the target, and the imaginary part describes excitation of the continuum. This allows us to take long-range polarization and short-range interaction of the incident electron and target into account in the calculation. These effects are expected to be very important in e-O scattering. The method has been successfully applied to the studies of resonance phenomena in electron impact on hydrogen [17] and sodium [18]. It also has been used to investigate various excitation cross sections in the collision of electron by oxygen at energies a few eV above the ionization threshold, and good agreements with experiments have been obtained [19,20]. The detailed description of the CCO method has been given in Ref. [10], and we briefly review the essential features in Sec. II.

II. FORMALISM AND CALCULATION DETAILS

The coupled integral equations are represented in momentum spaces:

$$\langle \mathbf{k}i|T_S|0\mathbf{k}_0\rangle = \langle \mathbf{k}i|V_S^{(Q)}|0\mathbf{k}_0\rangle + \sum_{j\in P}\int d^3q\,\frac{\langle \mathbf{k}i|V_S^{(Q)}|j\,\mathbf{q}\rangle\langle \mathbf{q}j|T_S|0\mathbf{k}_0\rangle}{(E^+-\varepsilon_j-q^2/2)}, \quad (1)$$

where i, j represent target states; P projects a finite set of target states, including the ground state 0; and Q projects the continuum and the remaining discrete states. The subscript S indicates the total spin. $V_S^{(Q)}$ consists of two parts, the electron-target potential V_S and the complex, nonlocal polarization potential $W_S^{(Q)}$,

$$V_S^{(Q)} = V_S + W_S^{(Q)}. \quad (2)$$

*yajunzhou2003@yahoo.com.cn

The basic approximation for the matrix element of $W_S^{(Q)}$ is

$$\langle \mathbf{k}'i|W_S^{(Q)}|j\mathbf{k}\rangle = \int d^3q' \int d^3q \times \frac{\langle \mathbf{k}'i|V_S|\psi^{(-)}(\mathbf{q}_<)\mathbf{q}_>\rangle\langle \mathbf{q}_>\psi^{(-)}(\mathbf{q}_<)|V_S|j\mathbf{k}\rangle}{E^{(+)} - q^2/2 - q'^2/2}. \tag{3}$$

Here $\mathbf{q}_<$ and $\mathbf{q}_>$ represent the lesser and greater of q and q' of the absolute momenta of the outgoing particles, respectively, and $\langle \mathbf{r}|\psi^{(-)}(\mathbf{q}_<)\rangle$ is a Coulomb wave orthogonalized to the orbital from which the electron is removed. $\langle \mathbf{r}|\mathbf{q}_>\rangle$ is a plane wave. This approximation accounts for the Coulomb screening effect for the ejected electron.

The direct potential matrix element is calculated by an analytic form. The exchange matrix element has a similar analytic form in the equivalent-local approximation and angular momentum projection approximation that are made for the whole polarization potential. The polarization potential element is then calculated in the variable K

$$\langle \mathbf{k}'i|W_S^{(Q)}|j\mathbf{k}\rangle = \sum_{l'',m''} i^{l''} C_{l''l'l}^{m''m'm} U_{l''l'l}(K) Y_{l''m''}(\hat{\mathbf{K}}), \tag{4}$$

where lm and $l'm'$ are the orbital angular momentum quantum numbers of the states i and j, respectively, and

$$\mathbf{K} = \mathbf{k} - \mathbf{k}'. \tag{5}$$

The half-on-shell approximation

$$\tfrac{1}{2}k^2 = E - \varepsilon_j \tag{6}$$

is made for the amplitudes (3), reducing the computation of the optical potential to the function $U_{l''l'l}(K)$ obtained by inverting (4).

$$U_{l''l'l}(K) = \sum_{m'',m'} C_{l''l'l}^{m''m'm} \int d\hat{\mathbf{K}} \langle \mathbf{k}'i|W_S^{(Q)}|j\mathbf{k}\rangle i^{-l''} Y_{l''m''}^*(\hat{\mathbf{K}}). \tag{7}$$

The present calculation was carried out by using the same quadrature points for solving the integral equation (1) over a range of energies, thus making the off-shell potential matrices energy independent. We calculated the slowly varying optical potentials at a few energy points instead of the whole energy range. For computation, we make a partial-wave expansion of the T_S and $V_S^{(Q)}$ matrix elements, defining the partial matrix elements

$$\langle k'n'l'L'||T_{JS}||Llnk\rangle \tag{8}$$

for total orbital angular momentum quantum number J by

$$\langle \mathbf{k}'i|T_S|j\mathbf{k}\rangle = \sum_{L,M,L',M',J,K} \langle \hat{\mathbf{k}}'|L'M'\rangle C_{L'l'J}^{M'm'K} \times \langle k'n'l'L'||T_{JS}||Llnk\rangle C_{LlJ}^{MmK} \langle LM|\hat{\mathbf{k}}\rangle, \tag{9}$$

where

$$\langle \hat{\mathbf{k}}|LM\rangle \equiv Y_{LM}(\hat{\mathbf{k}}) \tag{10}$$

and C_{LlJ}^{MmK} is a Clebsch-Gordan coefficient. The definition of

$$\langle k'n'l'L'||V_{JS}^{(Q)}||Llnk\rangle \tag{11}$$

is analogous to (8) with $V_S^{(Q)}$ substituted for T_S.

The total cross section is then obtained by summing the partial-wave cross sections:

$$\sigma_{ij} = (2\pi)^4 \frac{k_i}{k_k} \frac{\widehat{S}^2}{\widehat{l}^2} \frac{1}{4\pi} \sum_{L,L',J} (2J+1)|\langle k'n'l'L'||T_{JS}||Llnk\rangle|^2. \tag{12}$$

The energies and widths of resonances for particular values of J and S have been found by fitting the Breit-Wigner form with a linear background

$$T_R = aE + b + \frac{c + id}{E - E_r + i\Gamma_R/2} \tag{13}$$

to the calculated partial wave T-matrix elements $\langle k'n'l'L'||T_{JS}||Llnk\rangle$ for each resonance over the resonant energy range, where E is the incident energy and E_R, Γ_R, a, b, c, and d are the fitting parameters. E_R is the resonant energy and Γ_R is the full width at half maximum.

In this Brief Report, we have calculated total cross sections in e-O collision from 9 to 11.4 eV. Up to 80 partial waves are included in the sum for the total cross sections. The calculation has been carried out at intervals of 5 meV (2 meV partly). In the present calculation, oxygen states are represented by single configuration wave functions which are obtained from the Hartree-Fock calculation for $1s^22s^22p^3nl$, and we treat $1s^22s^22p^2$ as a frozen core in their initial orbitals. We generate all valence nl orbitals in separate calculations for the individual $1s^22s^22p^3(^4S^o)nl$ states. The twelve lowest-lying discrete states of oxygen are included in P space for sufficient convergence. They are $2p^4\ ^3P$, $2p^33s\ ^3S^o$, $2p^33p\ ^3P$, $2p^34s\ ^3S^o$, $2p^33d\ ^3D^o$, $2p^34p\ ^3P$, $2p^35s\ ^3S^o$, $2p^34d\ ^3D^o$, $2p^35p\ ^3P$, $2p^36s\ ^3S^o$, $2p^35d\ ^3D^o$, and $2p^37s\ ^3S^o$. The optical potentials in Q space that describe the continuum are included in the couplings $2p$-$2p$, $2p$-$3s$, and $3s$-$3s$.

III. RESULTS AND DISCUSSION

The present calculated total cross sections are shown in Fig. 1, along with the only available absolute experimental data of Sunshine *et al.* [21]. Generally, the present results show good agreement with experimental data, which indicates the validity of the present CCO calculation. We also display the present first three partial waves calculations, namely

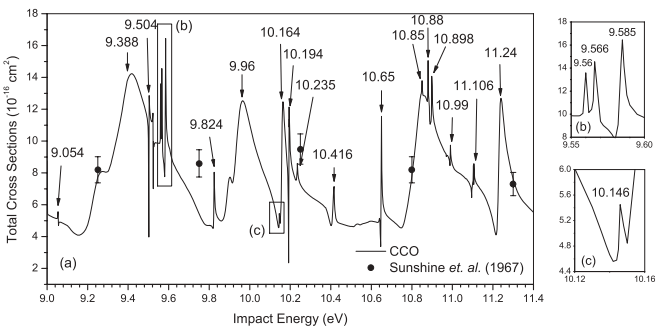

FIG. 1. The present CCO calculation of total cross sections for e-O collision from 9 to 11.4 eV, along with available experimental data of Sunshine *et al.* [21]. The intervals of present calculation were 5 meV (2 meV partly). Arrows are used to mark the centers of the resonance peaks.

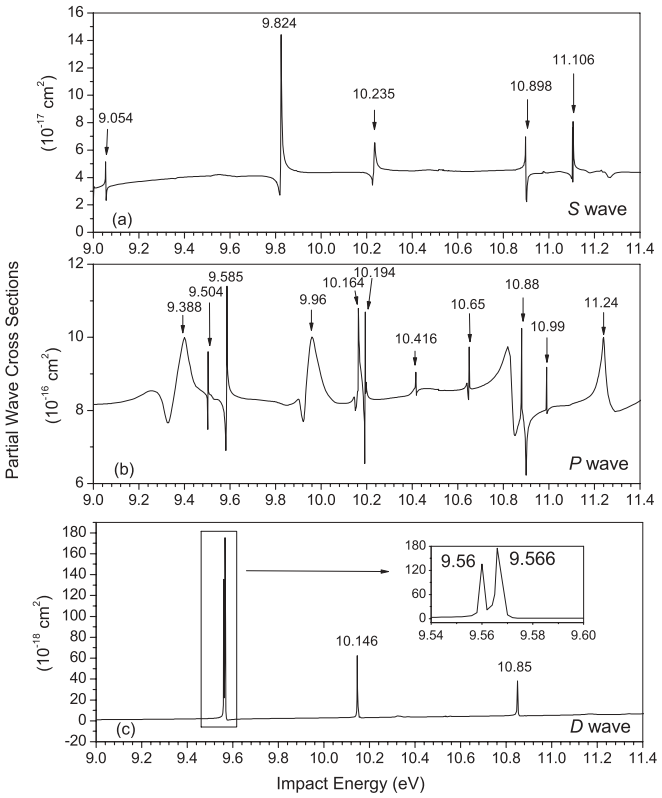

FIG. 2. Detailed (a) S, (b) P, and (c) D partial waves symmetries of the present CCO calculation for e-O collision from 9 to 11.4 eV at the intervals of 5 meV (2 meV partly). Arrows are used to mark the centers of the resonance peaks.

S ($J = 0$), P ($J = 1$), and D ($J = 2$) waves, in Fig. 2. All the resonances found in the present calculation are compared with available experimental observations and theoretical results in Table I.

Below the $3s$ excitation threshold of oxygen at 9.508 eV, the peak located at 9.504 eV with P-wave symmetry in the present calculation is in good agreement with the resonance at 9.5 eV which was confirmed by Edwards and Cunningham [4] and Matese [7]. Below the $3p$ excitation threshold at 10.974 eV, there are four resonances confirmed by previous investigations. They are the resonances at 10.63 [7] (10.73 [5]), 10.87 [4], 10.88 [7], and 10.90 eV [5]. The peaks at 10.65, 10.85, 10.88, and 10.898 eV in Fig. 1 should correspond to these confirmed resonances. It is shown from Fig. 2 that the peaks at 10.65 and 10.88 eV belong to the P-wave resonance, as well as the peaks at 10.85 and 10.898 eV belong to the D-wave resonance and S-wave resonance, respectively. According to the present model of configurations, the present confirmed Feshbach resonance features at 9.504, 10.65, 10.85, 10.88, and 10.898 eV should be associated with the negative-ion configurations of $2p^3(^4S^o)3s3p\ ^2P$, $2p^3(^4S^o)3p^2\ ^6P^o$, $2p^3(^4S^o)3p^2\ ^4D^o$, $2p^3(^4S^o)3p^2\ ^4S^o$, and $2p^3(^4S^o)3p^2\ ^2P^o$, respectively. The broader resonance feature at 9.96 eV of the present results with P-wave symmetry should coincide with the resonance at 9.94 eV of Rountree and Henry [8], while no feature has been found corresponding to the resonance at 9.67 eV [8] in the present calculation.

In addition to the resonances confirmed above, some new resonance features are also found in the present calculation displayed in both Figs. 1 and 2. The narrow peaks centered at 9.054, 9.824, 10.235, and 11.106 eV belong to S-wave

TABLE I. Configurations, energies, and widths for resonances in e-O collisions from 9 to 11.4 eV. All resonant energies (E_R) are in eV and are referenced to the ground state of the atomic oxygen. The unit of widths (Γ_R) is in meV.

	Present			Experimental		Theoretical	
Configurations	E_R (eV)	Γ_R (meV)	Partial waves	Edwards *et al.* [3,4]	Spence [5]	Matese *et al.* [6,7]	Rountree and Henry [8]
	9.054	0.95	S ($J = 0$)				
	9.388	48.48	P ($J = 1$)				
$2p^3(^4S^o)3s3p\ ^2P$	9.504	0.71	P ($J = 1$)	9.5		9.5	
	9.56	1.12	D ($J = 2$)				
	9.566	1.18	D ($J = 2$)				
	9.585	0.045	P ($J = 1$)				
	9.824	3.66	S ($J = 0$)				
	9.96	30.94	P ($J = 1$)				9.94
	10.146	1.25	D ($J = 2$)				
	10.164	11.94	P ($J = 1$)				
	10.194	1.60	P ($J = 1$)				
	10.235	3.76	S ($J = 0$)				
	10.416	0.29	P ($J = 1$)				
$2p^3(^4S^o)3p^2\ ^6P^o$	10.65	2.84	P ($J = 1$)		10.73	10.63	
$2p^3(^4S^o)3p^2\ ^4D^o$	10.85	1.52	D ($J = 2$)	10.87			
$2p^3(^4S^o)3p^2\ ^4S^o$	10.88	1.80	P ($J = 1$)			10.88	
$2p^3(^4S^o)3p^2\ ^2P^o$	10.898	1.88	S ($J = 0$)		10.90		
	10.99	0.62	P ($J = 1$)				
	11.106	0.48	S ($J = 0$)				
	11.24	19.02	P ($J = 1$)				

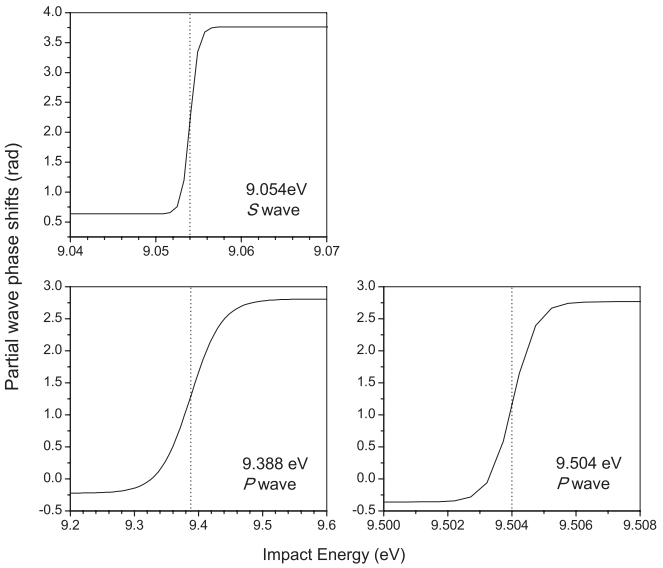

FIG. 3. Partial wave phase shifts of the present CCO calculated resonances in the elastic-scattering region. The dotted line is used to mark the position where the phase shift increases by $\pi/2$ in each case.

resonances, and the narrow peaks at 9.56, 9.566, and 10.146 eV belong to D-wave resonances. More resonance features belong to P-wave symmetry, including the narrow peaks at 9.585, 10.164, 10.194, 10.416, and 10.99 eV, as well as all the broader resonance features near 9.388 and 11.24 eV. To the best of our knowledge, these new resonance structures have not been reported by previous investigations. Note that atomic oxygen has a complicated open-shell structure, and its excitation channels start to open in this energy region. Thus there should be various doubly excited states associated with the present O^+ $2p^3(^4S^o)$ ion core. In Fig. 3, we have plotted the present calculation of elastic partial wave phase shifts as a function of energy near the resonance region. In each case of Fig. 3, the phase shift increases by π radians as the energy traverses the resonant energy position, which represents a complete description of resonant behavior.

IV. CONCLUSION

In this Brief Report, detailed CCO calculation of scattering cross sections have been presented for studying resonance phenomena in the process of electron impact on atomic oxygen in the energy region from 9 to 11.4 eV. The present results have shown agreements with available data of experimental and theoretical work. Most of known Feshbach resonances have been located and confirmed in the present calculation. New positions of resonances have been found and restricted to S, P, or D partial wave symmetries. However, more experimental and theoretical works are sincerely needed to investigate resonance phenomena in e-O collision over this energy region.

ACKNOWLEDGMENTS

This work is supported by the National Natural Science Foundation of China under Grant No. 10874035. One of us (Y. Wang) is grateful for the Project (HIT.NSRIF.2009161) Supported by Natural Scientific Research Innovation Foundation in Harbin Institute of Technology.

[1] G. J. Schulz, Rev. Mod. Phys. **45**, 378 (1973).
[2] S. J. Buckmam and C. W. Clark, Rev. Mod. Phys. **66**, 539 (1994).
[3] A. K. Edwards, J. S. Risley, and R. Geballe, Phys. Rev. A **3**, 583 (1971).
[4] A. K. Edwards, and D. C. Cunningham, Phys. Rev. A **8**, 168 (1973).
[5] D. Spence, Phys. Rev. A **12**, 721 (1975).
[6] J. J. Matese, S. P. Rountree, and J. W. Henry, Phys. Rev. A **7**, 846 (1973).
[7] J. J. Matese, Phys. Rev. A **10**, 454 (1974).
[8] S. P. Rountree and R. J. W. Henry, Phys. Rev. A **6**, 2106 (1972).
[9] I. E. McCarthy and A. T. Stelbovics, Phys. Rev. A **22**, 502 (1980).
[10] I. E. McCarthy and A. T. Stelbovics, Phys. Rev. A **28**, 2693 (1983).
[11] I. E. McCarthy, K. Ratnavelu, and A. M. Weigold, J. Phys. B **21**, 3999 (1988).
[12] I. E. McCarthy, K. Ratnavelu, and Y. Zhou, J. Phys. B **22**, 2597 (1989).
[13] M. J. Brunger, I. E. McCarthy, K. Ratnavelu, P. J. O. Teubner, A. M. Weigold, Y. Zhou, and L. J. Allen, J. Phys. B **23**, 1325 (1990).
[14] I. E. McCarthy and E. Weigold, Adv. At. Mol. Opt. Phys. **27**, 165 (1990).
[15] I. E. McCarthy, K. Ratnavelu, and Y. Zhou, J. Phys. B **24**, 4431 (1991).
[16] I. E. McCarthy, K. Ratnavelu, and Y. Zhou, J. Phys. B **26**, 2733 (1993).
[17] I. E. McCarthy and B. Shang, Phys. Rev. A **46**, 3959 (1992).
[18] L. Jiao, Y. Zhou, and Y. Wang, Phys. Rev. A **81**, 042713 (2010).
[19] Y. Wang, Y. Li, and Y. Zhou, Chin. Phys. Lett.**22**, 87 (2005).
[20] Y. Wang and Y. Zhou, J. Phys. B **39**, 3009 (2006).
[21] G. Sunshine, B. B. Aubrey, and B. Bederson, Phys. Rev. **154**, 1 (1967).